SOCS3 is a modulator of human macrophage phagocytosis

Peter Gordon, Blessing Okai, Joseph I. Hoare, Lars P. Erwig, and Heather M. Wilson[1]

School of Medicine, Medical Sciences and Nutrition, University of Aberdeen, Institute of Medical Sciences, Foresterhill, Aberdeen, United Kingdom

ABSTRACT

Suppressor of cytokine signaling (SOCS) proteins are recognized as key feedback inhibitors modulating the inflammatory activities of macrophages, but comparatively little is known about whether and how they affect phagocytosis. Here, we evaluated the role of SOCS3 in driving the inflammatory phenotype and phagocytic uptake of apoptotic cells by human macrophages and the signaling pathways that are necessary for efficient phagocytosis. In M1-activated human monocyte-derived macrophages, SOCS3 silencing, using short interfering RNA technology, resulted in a decreased expression of proinflammatory markers and an increased expression of M2 macrophage markers. Strikingly, we demonstrated for the first time that SOCS3 knockdown significantly enhances the phagocytic capacity of M1 macrophages for carboxylate-modified beads and apoptotic neutrophils. With the use of live-cell video microscopy, we showed that SOCS3 knockdown radically affects the temporal dynamics of particle engulfment, enabling more rapid uptake of a second target and delaying postengulfment processing, as evidenced by deferred acquisition of phagosome maturation markers. SOCS3 knockdown impacts on phagocytosis through increased PI3K and Ras-related C3 botulinum toxin substrate 1 (Rac1) activity, pathways essential for engulfment and clearance of apoptotic cells. Enhanced phagocytosis in SOCS3-silenced cells was reversed by pharmacological PI3K inhibition. Furthermore, we revealed that actin polymerization, downstream of PI3K/Rac1 activation, was significantly altered in SOCS3-silenced cells, providing a mechanism for their greater phagocytic activity. The findings support a new model, whereby SOCS3 not only plays an important role in driving macrophage inflammatory responses but modulates key signaling pathways organizing the actin cytoskeleton to regulate the efficiency of phagocytic processes. *J. Leukoc. Biol.* **100: 771–780; 2016.**

Introduction

Macrophages are highly heterogeneous cells that can adopt many phenotypes and functions to shape immune responses and maintain and restore tissue homeostasis. The properties macrophages develop are determined by integration of signals from their microenvironment. Microbial products and IFN-γ (M1 activation), for example, can drive proinflammatory, microbicidal, and tumoricidal macrophages, whereas IL-4 (M2 activation) results in anti-inflammatory, tissue-healing macrophages [1, 2]. These are, however, extremes on a continuum of the phenotypes found in vivo. A recent macrophage classification has now been proposed based on their activation conditions and provides a common framework for macrophage activation nomenclature [3]. A fundamental function of macrophages for conserving homeostasis and resolving inflammation is engulfment and clearance of apoptotic cells [4–7]. This uptake results in production of anti-inflammatory cytokines, including TGF-β and IL-10 [8], which inhibits inflammatory mediator production, further dampening the inflammation (reviewed in ref. [6]). Failure of apoptotic cell clearance promotes secondary postapoptotic necrosis with release of proteolytic enzymes and other inflammatory molecules [9]. As such, defective apoptotic cell clearance, especially apoptotic neutrophils, impedes resolution and can lead to the development of autoimmunity or inflammatory diseases, such as rheumatoid arthritis and pulmonary fibrosis. Therapeutic approaches designed to enhance macrophage clearance of apoptotic cells could therefore improve the resolution of inflammation. Recognition of apoptotic cells by macrophages activates several signaling cascades, including Rac1, causing actin reorganization and cell engulfment [10, 11]. However, the intracellular mechanisms and pathways controlling

---

Abbreviations: CRIB = Cdc42/Rac1-interactive binding motif, CTCF = corrected total cell fluorescence, F-actin = filamentous (polymerized) actin, FAK = focal adhesion kinase, LAMP-1 = lysosomal-associated membrane protein 1, MARCO = macrophage receptor with collagenous structure, MRC1 = macrophage mannose receptor 1, p-Akt = phospho-Akt, PAK = p21-activated kinase, PI = phagocytic index,

(continued on next page)

The online version of this paper, found at www.jleukbio.org, includes supplemental information.

their activity are not well defined, especially in primary human macrophages.

SOCS are a widely expressed family of intracellular proteins [SOCS1–7 and cytokine-inducible Src homology 2 domain-containing protein (CIS)] with important roles in immune regulation [12–15]. They are best known for their negative-feedback inhibition of the JAK-STAT pathways but also regulate other signaling cascades, including PI3K, MAPK, and NF-κB pathways [12–15]. We [16–18] and others [19–21] have shown that SOCS proteins, especially SOCS1 and SOCS3, are critical in regulating the pro- and anti-inflammatory functions of macrophages both in vivo and in vitro. Expression of SOCS1 and SOCS3 is rapidly up-regulated by a variety of stimuli, and they each have distinct roles in shaping macrophage functions. SOCS1 is best known for its role in inhibiting IFN-γ and TLR4 signaling, and SOCS1 knockout mice die from neonatal fatal inflammatory disease, where IFN-γ is the chief cause of the resultant pathology [22–24]. By contrast, SOCS3 regulates signaling mediated by the common IL-6R family subunit gp130 to limit IL-6-induced STAT1 gene expression and inhibit IL-6-induced STAT3 anti-inflammatory effects [25–27]. In SOCS3-deficient murine macrophages, IL-6 behaves more like the immunosuppressive cytokine IL-10, through prolonged STAT3 activation and suppression of LPS signaling [27]. We [17, 18] and others [28, 29] have previously shown that rodent M1 macrophage activation, in vitro and in vivo, is strongly associated with increased SOCS3 expression that controls proinflammatory functions. However, the effects of SOCS3 expression on regulating human macrophage phenotypes and their specific functions—for example, phagocytic efficiency—have not been determined.

Here, we examined the hypothesis that SOCS3 is important in controlling pathways driving phagocytosis, and its deficiency enhances uptake of apoptotic cells in human macrophages. Our results show that macrophage SOCS3 limits phagocytic uptake via inhibition of a unique PI3K/Rac1/actin remodeling pathway. They provide new insights into the role of SOCS3 in macrophage phagocytosis of apoptotic cells and suggest that up-regulation of SOCS3 expression in the initial stages of inflammation could inhibit apoptotic cell uptake and early switching of macrophage function, thus driving an efficient inflammatory response.

MATERIALS AND METHODS

Cell isolation

Human monocyte-derived macrophages and neutrophils were isolated from blood of healthy adult-consenting donors, as approved by the Ethics Review Board of the College of Life Science & Medicine, University of Aberdeen. Neutrophils and PBMCs were fractionated by density gradient centrifugation. Monocytes were isolated from the PBMCs by positive selection using human CD14 microbeads to ensure a highly purified population (Miltenyi Biotec, Bergisch Gladbach, Germany) and differentiated into macrophages over 7 d in DMEM (Lonza, Basel, Switzerland), supplemented with 1% L-glutamine, 2% penicillin/streptomycin (GE Healthcare Life Sciences, Buckinghamshire,

United Kingdom) and 10% human AB+ serum [18], using current experimental guidelines [3].

Gene silencing

Knockdown experiments were performed using predesigned and validated siRNA for SOCS3 (s17191; Thermo Fisher Scientific Life Sciences, Waltham, MA, USA) or a nontargeting siRNA sequence control (4390844; Thermo Fisher Scientific Life Sciences). Macrophages were transfected using Lipofectamine RNAiMAX (Thermo Fisher Scientific Life Sciences) in serum-free medium, according to the manufacturer's instructions, as described previously [18]. In brief, at d 8 of differentiation, macrophages were plated in antibiotic-free medium and transfected. After overnight incubation, the medium was supplemented with antibiotics and cells incubated at 37°C for 48 h before treatment. SOCS siRNA transfection efficiency was 89 ± 9%, as determined by counts for the number of macrophages containing fluorescently tagged siRNA (Thermo Fisher Scientific Life Sciences). Knockdown efficacy was analyzed by means of PCR and Western blotting and was typically 75–90% (Supplemental Fig. 1). For scoring of effects of SOCS3 knockdown on individual cells, at least 100 cells were analyzed to ensure that the majority analyzed had effective silencing. The transfection procedure does not interfere with the phagocytic abilities of the cell, as determined by a comparison among control, siRNA-transfected cells, mock transfected cells (Lipofectamine RNAiMAX only), and nontransfected control cells.

RNA extraction and quantitative RT-PCR

Total cellular RNA was isolated from untreated or cytokine-stimulated human monocyte-derived macrophages using Trizol extraction reagent (Thermo Fisher Scientific Life Sciences), followed by RNA clean-up using an RNeasy Mini Kit (Qiagen, Germantown, MD, USA), according to the manufacturer's instructions. A total of 5 μg from each sample was reverse transcribed using the First Strand cDNA Synthesis Kit and Oligo(dT) 15 Primer (Promega, Southampton, United Kingdom) and SuperScript II (Thermo Fisher Scientific Life Sciences), as recommended by the manufacturers. For each gene, the PCR was performed on 50, 100, and 200 ng of the cDNA using the following primers: TNF-α forward (cgctccccaagaagacag), TNF-α reverse (agaggctgag-gaacaagcac); SOCS3 forward (cttcgactgcgtgctcaa), SOCS3 reverse (gtaggtggc-gaggggaag); IL-6 forward (gatgagtacaaaagtcctgatcca), IL-6 reverse (ctgcagccactggttctgt); HLA-DR forward (acaactacggggttgtggag), HLA-DR reverse (gctgcctggatagaaaccac); TGM2 forward (ggcaccaagtacctgctca), TGM2 reverse (agaggatgcaaagaggaacg); MRC1 forward (ttcagaaggttttacttggagtga), MRC1 reverse (tctccataagcccagtttttca); SOCS1 forward (cccctggttgttgtagcag), SOCS1 reverse (gtaggaggtgcgagttcagg); MARCO forward (ggaaactggaactagg-gagaga), MARCO reverse (cctcccgaagtcacctttact). Quantitative real-time PCR was carried out by LightCycler 480 (Roche Diagnostics, West Sussex, United Kingdom) with the Universal Probe Library system (Roche Diagnostics). Gene expression was analyzed using the comparative threshold method with target gene mRNA levels being normalized to GAPDH and hypoxanthine phosphoribosyltransferase. Data are expressed as fold-change differences in gene levels in SOCS3 siRNA-transfected cells compared with that of transfected with control, nontargeting siRNA.

Phagocytosis assays

Phagocytosis assays of latex beads or apoptotic neutrophils were performed in SOCS3 siRNA or scrambled control siRNA-transduced macrophages, activated with 100 ng/ml LPS and 20 ng/ml IFN-γ for 3 h. Carboxylate-modified latex beads were used as simplified targets that mimic the surface charge of apoptotic cells. Neutrophils were separated from whole blood using Histopaque (Sigma-Aldrich, Irvine, United Kingdom) density gradient centrifugation (#1119 and #1077). Apoptotic neutrophils were obtained by culturing neutrophils in RPMI for 1 d, which typically resulted in >70% apoptotic cells, as determined by Annexin V and propidium iodide staining. Macrophages were labeled with Vybrant DiD (Thermo Fisher Scientific Life Sciences) and apoptotic neutrophils with Vybrant DiO (Thermo Fisher Scientific Life Sciences) as recommended by the manufacturer. For uptake

---

(continued from previous page)

Rac1 = Ras-related C3 botulinum toxin substrate 1, siRNA = short interfering RNA, SOCS = suppressor of cytokine signaling, TGM2 = transglutaminase 2

assays, 10 μm carboxylated polystyrene beads (Polysciences, Eppelheim, Germany) were added to macrophages at a ratio of 3:1 (bead:macrophage); for apoptotic neutrophil assays, cells were added at a ratio of 10:1 (apoptotic neutrophils:macrophage). At the end of the incubation period, typically 3 h after bead/neutrophil addition, nonengulfed cells were removed by washing. Macrophages were fixed in 4% paraformaldehyde and the percentage of macrophages phagocytosing at least 1 bead/apoptotic neutrophil (green fluorescence) determined. PI was calculated as the mean number of beads or apoptotic neutrophils per 100 phagocytosing macrophages and provides an indication of the phagocytic efficiency of the macrophages. At least 100 macrophages were designated for analysis. In selected experiments, macrophages were preincubated with the PI3K inhibitor LY294002 (10 μM), 1 h before bead addition and determination of percent phagocytosis and PI. Incubation with DMSO served as vehicle control.

Phagosome maturation

To quantify phagosome maturation in SOCS3 knockdown macrophages, 10 μm polystyrene beads were added at a ratio of 3:1, following 3 h activation with LPS and IFN-γ. Cells were washed in ice-cold PBS and fixed for 15 min in 4% paraformaldehyde and permeabilized with 0.1% Triton X-100. Cells were blocked in 10% milk powder, 0.3% Tween-20 in PBS, and then fluorescently stained with the late phagosome maturation marker LAMP-1 for 1 h at room temperature. Cells were imaged using a Zeiss Axio Observer Z1 inverted microscope (Carl Zeiss AG, Oberkochen, Germany) with a mature phagosome defined as a "halo"-like ring surrounding an ingested bead, as previously described by our laboratory [30]. Maturation was then calculated as the number of mature rings divided by total beads ingested, multiplied by 100.

Live-cell imaging

Human monocyte-derived macrophages were cultured at 1.2×10^5 cells/well in ibidi 8-well, glass-bottom μ-slides (Thistle Scientific, Uddingston, United Kingdom). Time-lapse images were acquired over a 3 h period postbead/cell addition using an UltraVIEW VoX spinning disk microscope (Nikon, Surrey, United Kingdom). Images were captured at 1 min intervals using ×20 magnification at 37°C with an electron-multiplying, charge-coupled device back camera C9100-50 (Hamamatsu, Shizouka, Japan) and Volocity software (6.3 software; Improvision, PerkinElmer, Coventry, United Kingdom). Cells were bathed in CO_2 independent media (Thermo Fisher Scientific Life Sciences) while imaging. Videos were first optimized, keeping adjustments constant for every video and exported for quantification in ImageJ (Cell Counter and Chemotaxis plugins; NIH, Bethesda, MD, USA). More than 100 macrophages were selected and followed individually for each experiment. The percentage phagocytosis was calculated from the numbers of macrophages that contained a fully engulfed bead or demonstrated green fluorescence from ingested neutrophils; PI was calculated as above. At the end of each video, the number of beads engulfed by individual macrophages was counted and graphed according to the percentage of macrophages engulfing a defined number of beads. For distribution of neutrophil uptake, the maximum CTCF was determined per movie and divided into 10% groups. The CTCF of each phagocytosing macrophage was quantified and allocated into these percentiles, producing a distribution of CTCF levels. For quantifying macrophage motility, cells were picked at random at the beginning of each individual movie and their movement tracked using ImageJ (NIH) or Volocity 6.3 image analysis software (Improvision, PerkinElmer), measuring total distance traveled [the total length (micrometers) of the trajectory that the cell has migrated]; Euclidian distance [the straight-line distance (micrometers) between the position of the cell at the start (T = 0) and the end of the migration assay]; average velocity [the total distance migrated (micrometers)/time in hours]; and the directionality of cell movement (Euclidian distance/total distance traveled). Uptake speed of the first and subsequent beads was quantified from the time of first contact of the macrophage with a bead until the bead was fully enveloped.

Western blotting

Protein lysates were prepared from SOCS3 knockdown or control, scrambled siRNA-transduced macrophages, following 3 h activation with LPS and IFN-γ and 1 h with 10 μm carboxylated-modified polystyrene beads. A total of 20 μg protein was separated by SDS-PAGE and transferred to the Hybond-P polyvinylidene difluoride membrane (Amersham, GE Healthcare, Pittsburgh, PA, USA) for Western blot analysis with specific primary antibodies for Akt and p-Akt ser473 (Cell Signaling Technology, Danvers, MA, USA), SOCS3 (Abcam, Cambridge, United Kingdom), and β-actin (Sigma-Aldrich). Immunolabeled proteins were detected using appropriate HRP-conjugated secondary antibodies, followed by visualization with ECL (GE Healthcare). Bands were normalized to β-actin.

Pulldown assay for Rac1 activation

To detect active, GTP-bound Rac1, a pulldown assay using a Rac1 activation assay kit was performed, according to the manufacturer's instructions (Abcam). In brief, human macrophages were treated with 100 ng/ml LPS, 20 ng/ml IFN-γ, and carboxylated modified beads for 30 min, and the cells were lysed in a Rac1 lysis buffer containing protease inhibitors and GST-PAK-CRIB, a GST fusion of CRIB of PAK that selectively precipitates the activated form of Rac1. Extracts from unstimulated and nontransfected cells were spiked with Rac1-GDP and Rac1-GTP-γ-S to serve as controls for the specificity of the affinity purification. The spikes were incubated at 30° for 15 min with constant agitation, samples centrifuged, and the supernatant harvested for determination of Rac1 activation. Lysate (40 μl) was collected for total Rac1, which was used as an internal loading control for active Rac1. Glutathione-Sepharose beads were added to the remaining sample lysates and incubated for 30 min under constant mixing at 4°C. The beads and precipitated proteins were washed 3 times with ice-cold lysis buffer. The resulting pulldown (active Rac1) and total Rac1 was then immunoblotted with Rac1 antibody, according to the manufacturer's instructions, and immunoblotted proteins were detected using an ECL-based detection system (GE Healthcare).

Live imaging of actin cytoskeleton

Human monocyte-derived macrophages transfected with control, scrambled siRNA or SOCS3 siRNA were labeled using an SiR-Actin detection probe (Spirochrome, Stein am Rhein, Switzerland) for live-cell imaging of the cytoskeleton, based on a silicon rhodamine fluorophore and the F-actin-binding small molecule, jasplakinolide [31]. Live-cell staining was attained by adding 500 nM of the probe to DMEM complete medium and incubated at 37°C in a 5% CO_2 incubator for 2 h before imaging. Macrophages were treated with 100 ng/ml LPS and 20 ng/ml IFN-γ. Immediately before imaging, DMEM was replaced with 2 ml prewarmed, supplemented CO_2-independent media (Thermo Fisher Scientific Life Sciences) containing 10 μm carboxylate-modified beads at a 3:1 beads:macrophage ratio. Images were captured by Volocity 6.3 software (Improvision, PerkinElmer) every minute over a 3 h period. At least 3 independent experiments were performed with a minimum of 4 movies per experiment. For reliable quantification, all images were captured with the same camera setting (Ultraview 640 nm laser power, exposure time, and back camera sensitivity). In selected experiments, cells were fixed with 4% paraformaldehyde, labeled with SiR-Actin, and Z stacks obtained using a ×40 oil objective and a Zeiss LSM 710 confocal microscope. Maximum intensity projections were generated from the acquired 3-dimensional images using Zen software. From each independent experiment, at least 30 macrophages were randomly selected for quantification of macrophage area and mean fluorescence intensity analysis and calculated using ImageJ software.

Statistics

Statistical analyses were performed using GraphPad Prism 5. Student's 2-tailed *t* tests were performed, where appropriate, to assess the significance of differences. In the absence of normal distribution, significance was determined by a Mann-Whitney and Wilcoxon signed-rank tests. Uniform or random distribution was assessed using the Rayleigh distribution test.

RESULTS

SOCS3 knockdown alters the expression of inflammatory markers and increases phagocytosis in human monocyte-derived macrophages

Previous studies have shown SOCS3 to be important in controlling the inflammatory status of rodent macrophages and their ability to prime and induce T cell responses [17–19]. Our initial experiments determined whether SOCS3 also plays a role in directing the phenotypic characteristics of M1-activated human monocyte-derived macrophages by SOCS3 silencing and gene expression analysis of macrophage markers. SOCS3 knockdown results in a decrease in expression of proinflammatory genes (TNF, IL-6, HLA-DR), while enhancing those markers associated with M2 macrophages (mannose receptor, TGM2, and SOCS1); by contrast, MARCO showed a minimal change in expression levels (**Fig. 1** and Supplemental Fig. 1A–D). Therefore, these results confirm the efficiency of our knockdown system and the importance of SOCS3 in driving specific proinflammatory characteristics of human macrophage.

A key function of macrophages in regulation of inflammation is efficient clearance of apoptotic cells that subsequently induces characteristics of M2 anti-inflammatory macrophages [6, 8, 32]. To evaluate whether SOCS3 has a significant influence on this central macrophage function, human monocyte-derived macrophages, with or without SOCS3 silencing, were cultured with carboxylate-modified latex beads as a surrogate target mimicking the surface charge of apoptotic cells and the phagocytic ability determined 1 h postbead addition [7]. Strikingly, there was a modest but statistically significant increase in the percentage of macrophages phagocytosing beads after SOCS3 knockdown compared with those transfected with control siRNA (**Fig. 2A** and **D**), with a mean increase in uptake rate of $28.5 \pm 8.1\%$ over control. Macrophage preparations from every human donor tested ($n = 6$) displayed such increased phagocytic responses. There was a corresponding significant increase in the PI after SOCS3 knockdown, increasing, on average, by $47.7 \pm 13.2\%$ over that of control siRNA-transfected cells (Fig. 2B and E). Following uptake, the engulfed particles are trafficked into a series of increasingly acidified membrane-bound structures, leading to phagosome maturation and particle degradation [7, 33]. There is growing evidence that the rate and extent of phagosome maturation differ with the activation state of the macrophage [34]. Here, we found that phagosome maturation, as identified by acquisition and staining with the classic late maturation marker LAMP-1 [30], was delayed in SOCS3-silenced cells (Fig. 2C and F), with a $24.2 \pm 3.5\%$ decrease, again highlighting the importance for SOCS3 in controlling this process.

We next established detailed kinetics of the increase in phagocytosis in SOCS3 knockdown macrophages compared with control siRNA-transfected macrophages by using time-lapse live-cell imaging and confocal microscopy to follow uptake of carboxylate-modified beads or the more physiologic substrate of apoptotic neutrophils. **Figure 3A** and **B** (and Supplemental Videos 1 and 2) show exemplary events of macrophages migrating toward beads or apoptotic cells, respectively, and their subsequent engulfment. A significant increase in bead uptake was observed after 1 h incubation in SOCS3 knockdown
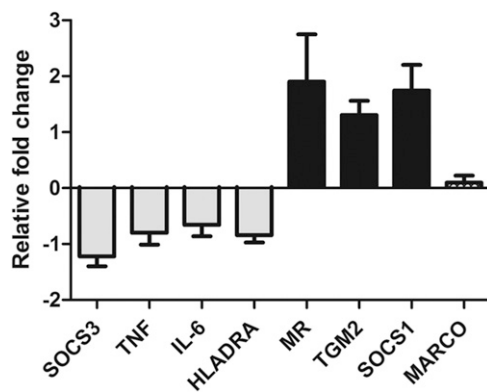

Figure 1. SOCS3 silencing decreased M1 and increased M2 macrophage inflammatory markers. Human monocyte-derived macrophages were transfected with control scrambled siRNA or SOCS3-specific siRNA and activated by IFN-γ/LPS for 6 h. mRNA expression was analyzed by quantitative PCR for the proinflammatory markers SOCS3, TNF, IL-6, HLA-DR, and MARCO and anti-inflammatory markers mannose receptor (MR), TGM2, and SOCS1. Values are normalized to a housekeeping gene (*GAPDH*) and shown as relative fold change in expression of genes in SOCS3 knockdown macrophages compared with control, nontargeting siRNA-transfected cells. Values are means ± SD; $n = 5$ different macrophage donor preparations.

macrophages, and this increase continued to persist over the 3 h time course of the experiment (Fig. 3C). The PI was also significantly enhanced in SOCS3 knockdown macrophages over time, confirming an increase in overall proficiency of phagocytosis in these cells (Fig. 3D). As with carboxylate-modified beads, there was a significant increase in the percentage phagocytosis (Fig. 3E) and PI (Fig. 3F) of apoptotic neutrophils over time in SOCS3 knockdown compared with control, siRNA-transfected cells; however, the significant difference in the uptake efficiency was observed much earlier, from 15 min postincubation. This early response with SOCS3 knockdown macrophages suggests that effects on phagocytosis were direct and not a secondary consequence of altered gene expression over the time scale examined.

To extend our analysis of the differences in rate of phagocytosis in SOCS3 knockdown macrophages, total numbers of carboxylic beads or apoptotic neutrophils taken up by individual macrophages over a 3 h period were recorded. Most macrophages engulfed more than 1 bead or apoptotic cell (**Fig. 4A** and **B**); however, in the SOCS3 knockdown group, there were, overall, larger numbers of beads engulfed, with only the SOCS3 knockdown macrophages engulfing ≥11 beads (Fig. 4A). This was also reflected when macrophages phagocytosed apoptotic neutrophils, with a higher number of SOCS3-silenced cells compared with control siRNA-transfected cells displaying enhanced fluorescence values, indicative of more engulfment (Fig. 4B). Collectively, these results demonstrate that SOCS3 expression is important in controlling the degree of phagocytosis, and without it, the levels and rate of uptake are improved.

SOCS3 silencing had no effect on macrophage mobility but did increase the kinetics of engulfment

A potential factor causing the increased phagocytosis observed in SOCS3-silenced macrophages is an alteration in the migration
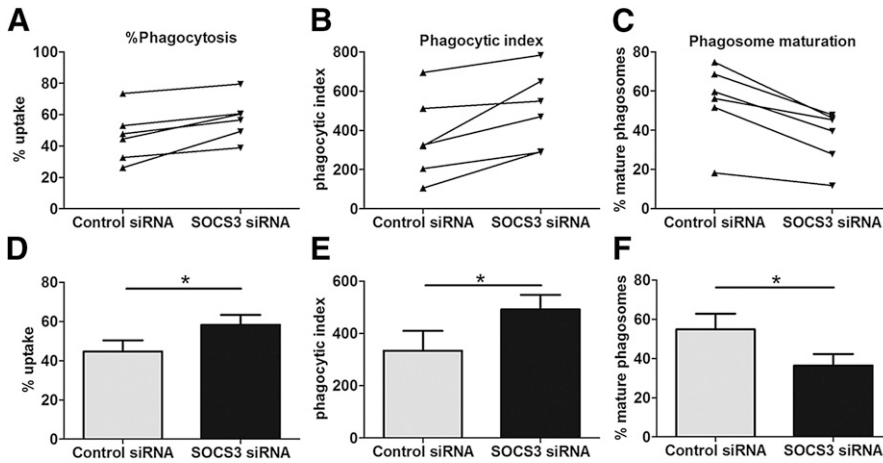
Figure 2. SOCS3 knockdown increases the percentage of macrophages phagocytosing and the PI and delays phagosome maturation. Human monocyte-derived macrophages were transfected with control scrambled siRNA or SOCS3-specific siRNA and incubated with carboxylate-modified latex beads. The percent of macrophages phagocytosing latex beads, the PI, and the percentage of macrophages containing mature phagosomes were determined after 1 h for 6 different donor macrophage preparation (A–C) and mean values ± SEM displayed (D–F). *P < 0.05.

or "search pattern" for their phagocytic target. Therefore, we determined the migratory kinetics of randomly selected macrophages over a 3 h uptake period. Quantitatively, there was no significant differences in total distance traveled (**Fig. 5A**), Euclidian distance (straight line distance between the macrophage and phagocytic substrate; Fig. 5B), or velocity of the cells

(Fig. 5C) observed for SOCS3 knockdown versus control siRNA-transduced macrophages. Moreover, there was no statistical difference in the directionality, a measure of migration randomness of the cells, as assessed using the Rayleigh uniformity test (Fig. 5D). Therefore, it was important to establish whether the increase in phagocytosis in the
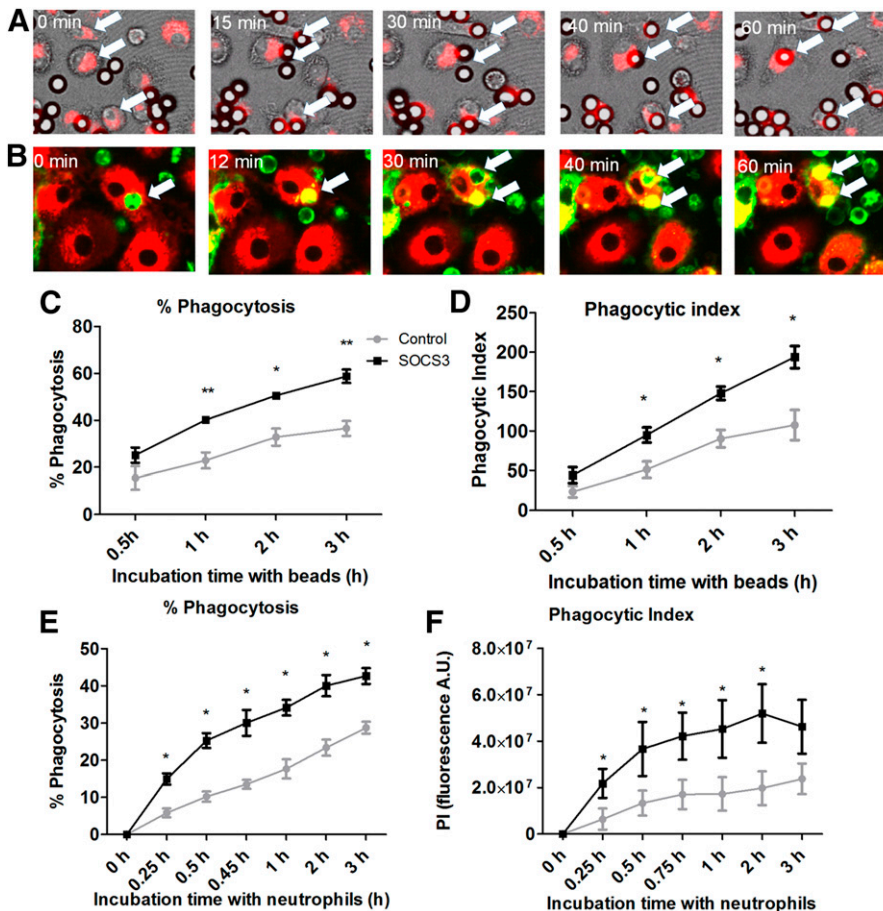

Figure 3. SOCS3 knockdown in human macrophages increases phagocytosis. Exemplary events of human macrophage migration toward their target and subsequent engulfment. Images were acquired from time-lapse video microscopy images during the incubation of LysoTracker Red-labeled human macrophages with carboxylate-modified latex beads (A) or Vybrant DiD-labeled macrophages (red) with green Vybrant DiO fluorescently labeled apoptotic neutrophils (B). The arrows indicate the uptake of beads (phagosomes gradually increased in fluorescence intensity after the particles were internalized) or apoptotic neutrophils over time in snapshot serial images. Engulfment was defined as membrane closure on the far side of the bead or the transfer of Vybrant DiO neutrophil dye (green) into the Vybrant DiD-labeled macrophage (red). Times displayed represent individual points from the start of the video monitoring uptake. The mean percentage of macrophages engulfing beads (C) and corresponding PI (D) or macrophages engulfing apoptotic neutrophil (E) and corresponding PI (F) in SOCS3 knockdown macrophages versus control siRNA-transfected cells. Means ± SEM. *P < 0.05, **P < 0.01; n = 6 individual donor macrophage preparations.

Figure 4. SOCS3 knockdown increases the phagocytic capacity of human macrophages. Percentage of macrophages that engulfed a defined number of carboxylate-modified beads (1–14) over a 3 h incubation period for SOCS3 knockdown cells (gray bars) or control siRNA-transfected macrophages (white bars; A). Percentage of macrophages that express a defined fraction of the maximum transferred green DiO apoptotic neutrophil dye, indicating uptake, over a 3 h incubation period (B), calculated as described in Materials and Methods. The figure is representative of results from 4 different macrophage preparations, and at least 100 macrophages were analyzed per preparation.
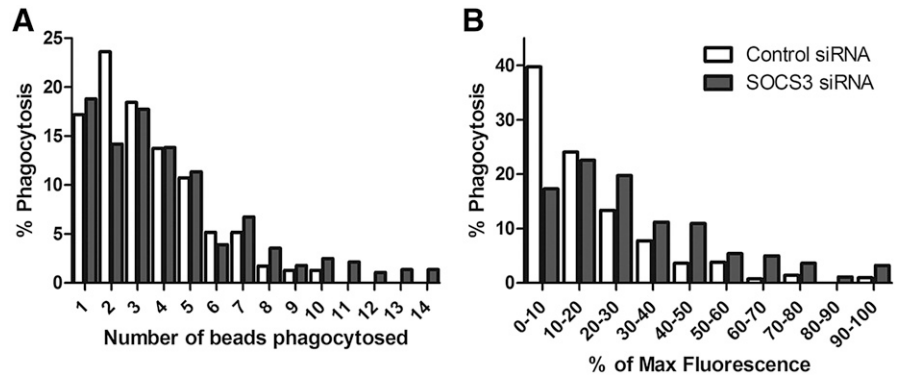

absence of SOCS3 was related to differences in speed of engulfment of specific targets; consequently, rates were examined. The engulfment time was defined as the time from first cell to target contact to complete internalization. Interestingly, there was no difference in the uptake rate of the first latex bead engulfed between SOCS3 or control siRNA-transfected macrophages (Fig. 5E); however, the rate of engulfment of subsequent beads was significantly faster in SOCS3 knockdown cells (Fig. 5F), suggesting that differences could relate to events controlling the remodeling of the actin cytoskeleton.

The depletion of SOCS3 enhances PI3K and Rac1 activity and downstream F-actin organization in human macrophages

Polymerization of F-actin at initial sites of phagocytosis is dependent on enrichment of phosphatidylinositol 4,5-bisphosphate in the inner leaflet of the plasma membrane, an event highly dependent on PI3K activity [11]. As SOCS proteins have been shown to inhibit PI3K activity in other cell systems [18, 35–37], we sought to determine whether silencing SOCS3 also affected this pathway in bead-activated macrophages by defining effects on p-AKT, a downstream substrate and surrogate marker of

Figure 5. Enhanced phagocytosis in SOCS3 knockdown macrophages is not a result of altered migration toward latex beads. Control siRNA-transfected or SOCS3 siRNA-transfected macrophages were selected randomly at the beginning of the phagocytosis videos and their movement tracked for 3 h using ImageJ tracking software at defined intervals. Total distance traveled (micrometers; A), Euclidian distance (straight line; micrometers; B), average cell velocity (micrometers/hour; C), and directionality of the cells (D) were calculated as in Materials and Methods. Values represent means ± SEM, $n = 6$ individual macrophage preparations. Engulfment speed of the first (E) and second (F) bead was quantified from the time of first contact of the macrophage with a bead until the bead was fully enveloped and compared in control siRNA-transfected and SOCS3 siRNA-transfected macrophages. ***$P < 0.001$.
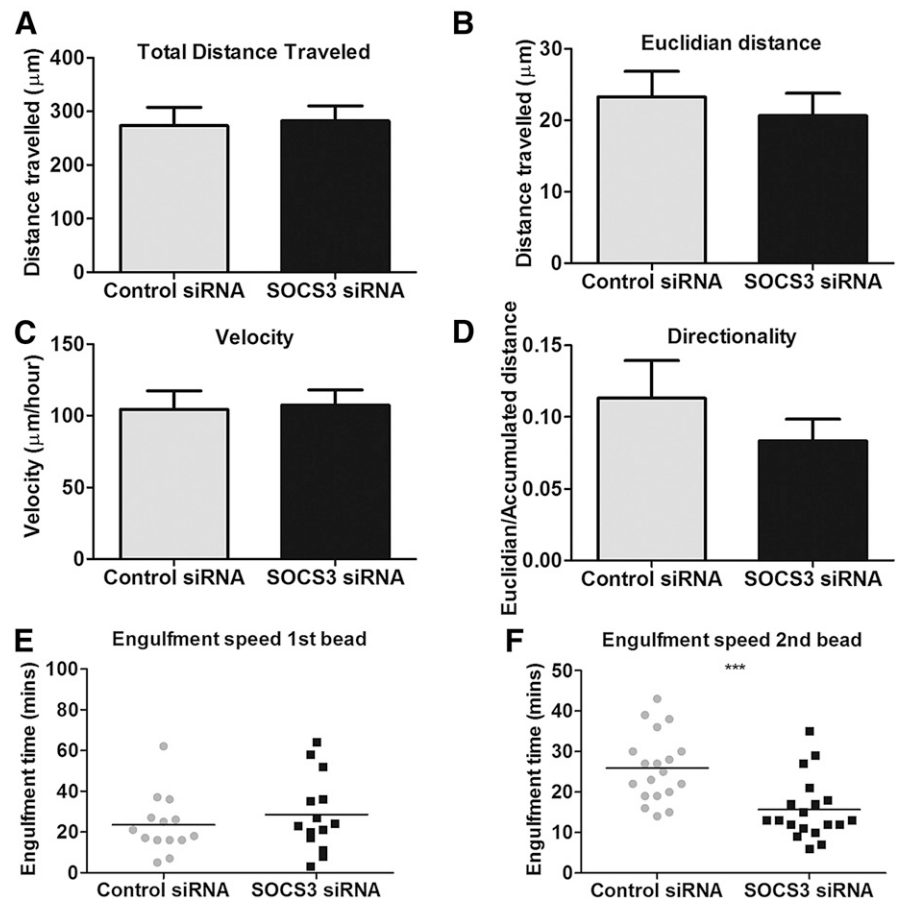
PI3K activity. On activation of phagocytosis with carboxylate-modified beads, there was a significant increase in p-AKT levels in SOCS3-silenced macrophages (**Fig. 6A**), supporting the view that the increase in phagocytosis observed in these cells is, at least in part, linked to an increase in PI3K-mediated actin cytoskeletal rearrangement. To determine whether this provided a molecular mechanism by which SOCS3 controls macrophage phagocytosis, we examined the effect of preincubation with the well-known PI3K inhibitor, LY294002. As previously shown, SOCS3 knockdown resulted in a significant increase in bead uptake (34.7 ± 8.3% increase) and PI (56.8 ± 7.1%). LY294002 preincubation inhibited baseline phagocytosis by 22.1 ± 0.9% in control, siRNA-transfected macrophages, in line with the importance of this pathway for bead uptake. PI3K inhibition also abrogated the significantly enhanced uptake observed in SOCS3-silenced macrophages compared with control, siRNA-transfected cells ($P = 0.231$; Fig. 6B) and abolished the increase in PI (Fig. 6C), confirming that PI3K is an essential component of the enhanced phagocytosis observed in SOCS3-silenced human macrophages.

PI3Ks interact with GTP-bound forms of the small GTPase, Rac1, that is key in regulating F-actin polymerization and reorganization of the actin cytoskeleton for internalization of apoptotic cells [38, 39]. To address whether SOCS3 silencing affected this pathway, we determined effects on Rac1 activity. Analysis of pulldown assays using the CRIB domain of PAK1 confirmed increased levels of active, GTP-bound Rac1 in SOCS3-silenced macrophages compared with control siRNA-transfected cells (Fig. 6D). Thus, PI3K activity and Rac1 activation are both augmented significantly in SOCS3-silenced human macrophages, conducive to the enhanced phagocytosis observed.

We next investigated whether cell morphology and actin polymerization/cytoskeletal arrangements were altered in SOCS3 knockdown macrophages as key downstream events of PI3K and Rac1 activity. Live imaging using a fluorogenic, cell-permeable probe, specific for F-actin [31], revealed that SOCS3 knockdown macrophages display a striking difference in morphology compared with control siRNA-transduced macrophages (**Fig. 7A** and **B**). On activation by latex beads, they exhibited a more polarized F-actin pattern and stress-fiber distribution at the cell periphery. By contrast control siRNA-transfected cells displayed a rounded morphology with a punctate actin arrangement. Moreover, SOCS3 knockdown macrophages showed an increase in cell size. These observations were verified following quantification of the macrophage body areas that demonstrate a significantly greater size in SOCS3 knockdown cells (Fig. 7C). Taken together, our results demonstrate greater activity of PI3K and Rac1 and subsequent actin polymerization following SOCS3 knockdown, providing a mechanistic insight into the enhanced rate of phagocytosis observed in these macrophages.

DISCUSSION

In this study, we demonstrate that SOCS3 is not only essential for controlling the proinflammatory phenotype of human monocyte-derived macrophages but is also a previously unidentified determinant regulating the efficiency with which they phagocytose apoptotic cells. We establish a novel mechanism of action, whereby SOCS3 alters important signaling pathways regulating uptake, with SOCS3 suppressing PI3K and Rac1 activity, as well as actin remodeling, to reduce the efficiency of phagocytosis. Thus,
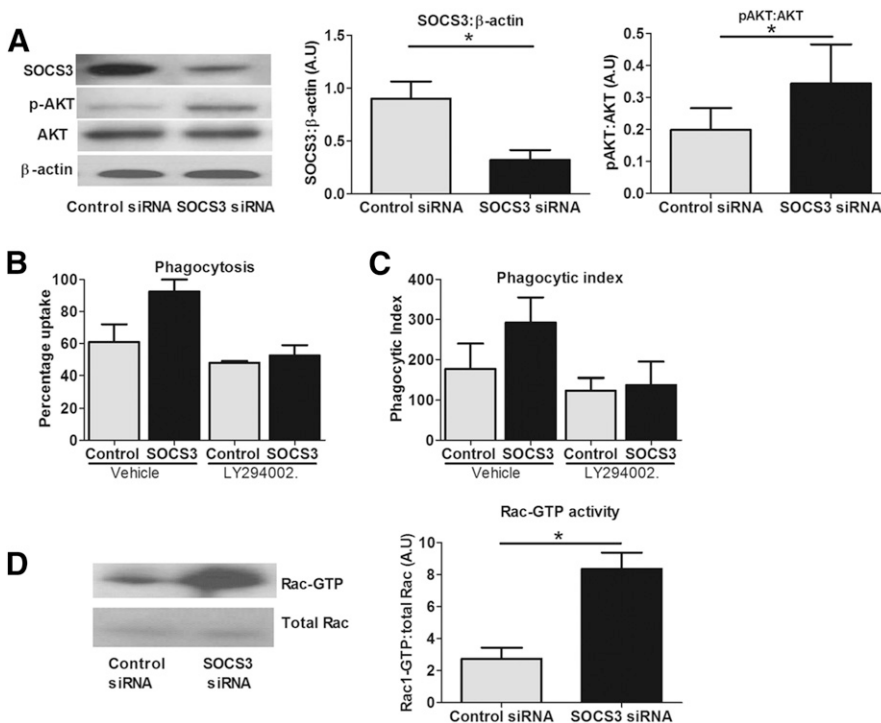

Figure 6. SOCS3 knockdown results in an increase in PI3K activity (p-AKT) and Rac1 activity on activation of phagocytosis with carboxylate beads. Human monocyte-derived macrophages were transfected with control siRNA or SOCS3 siRNA. Forty-eight hours following transfection, cells were stimulated with carboxylate-modified beads and PI3K activity assessed by Western blotting for downstream p-AKT. Blotting for SOCS3 confirmed knockdown. The figure shows expression of proteins, as determined by an immunoblot, representative of 3 individual experiments (A). Normalized densitometric analysis of scanned bands in arbitrary units (A. U.) for p-AKT and SOCS3. Incubation of SOCS3 knockdown macrophages for 30 min with the PI3K inhibitor LY294002 (10 μM) before addition of carboxylate-modified beads for 3 h abrogated the significant increase in phagocytic activity (B) and PI (C) in SOCS3 siRNA-transfected macrophages; DMSO (0.15%) served as a vehicle control. SOCS3 knockdown increases Rac1 activity, as shown by representative immunoblot after pulldown (D) and normalized densitometric analysis of scanned bands in arbitrary units for active Rac1:total Rac1, $n = 3$; *$P < 0.05$.
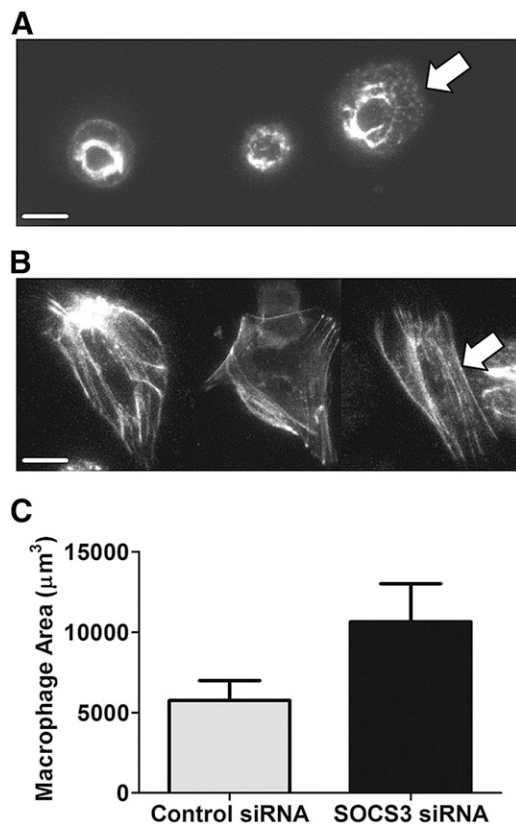
Figure 7. SOCS3 knockdown in human macrophages alters actin distribution, as determined by live-cell imaging. Human monocyte-derived macrophages transfected with control, scrambled siRNA (A) or SOCS3 siRNA (B) were fluorescently stained with SiR-Actin for live-cell imaging of the actin cytoskeleton. Images were captured every minute over a 3 h period. (A and B) Maximum intensity projections from 3-dimensional confocal images of fixed cells created from Z stacks using Zen software, also showing a punctate and polarized actin distribution (white arrows) for control siRNA- and SOCS3 siRNA-transfected cells, respectively. Original magnification, ×400. At least 3 independent experiments were performed with a minimum of 4 movies per experiment. Macrophages ($n \geq 30$) were randomly selected to determine macrophage area (micrometers). The cell-body area and perimeter were identified and measured using ImageJ on the captured images (C). Data are expressed as means ± SEM.

our studies uncover a new role for SOCS3 in controlling innate immune responses important in the resolution of inflammation.

Swift clearance of apoptotic cells is essential to preserve tissue integrity and prevent the accumulation of harmful products released from dying cells [9]. Deficient phagocytosis is associated with autoimmune diseases because of exacerbated and abnormal inflammatory responses [40]. Here, we demonstrate a consistent increase in uptake of different substrates by SOCS3-silenced macrophages, reflected in an enhanced PI. As clearance of apoptotic cells is such a critical event, even a modest increase in uptake, as was observed here, would be predicted to have important biologic effects on inflammation [9, 40]. It is well documented that proinflammatory stimuli inhibit uptake of apoptotic cells by M1 macrophages. Moreover, several studies have demonstrated that SOCS3 is potently up-regulated in M1

macrophages both in vitro and in vivo [12, 17–19, 29]. Our findings suggest that the M1-induced up-regulation of SOCS3 expression would play a role in inhibiting apoptotic cell uptake in the initial immune response and therefore, conserve proinflammatory functions for efficient pathogen killing [41]. Phagocytosis of apoptotic cells inhibits SOCS3 expression [42], and we propose that this inhibition would further boost the phagocytic capacity for apoptotic cells, as well as switch the macrophage toward a more anti-inflammatory phenotype. It is intriguing that the phagocytic capacity of SOCS3-deficient M1 murine macrophages for *Escherichia coli* was likewise enhanced compared with wild-type M1 macrophages; this suggests a common pathway for uptake of pathogens or apoptotic cells that can be inhibited by SOCS3 [19].

Live-cell imaging enabled us to analyze quantitatively the increase in uptake of both latex beads and apoptotic neutrophils in SOCS3-silenced macrophages. Strikingly, differences were noted between the engulfment kinetics of the 2 particles. The enhanced uptake of apoptotic neutrophils was observed much earlier than seen with beads, and most probably reflects the greater abundance of ligands that interact with phagocytic receptors on the latter. Uptake rates can reflect the initial recognition and interaction of macrophages with their substrate, and kinetic studies permitted calculations of the migration rate of macrophages toward their substrate, the distance traveled for interaction, and the overall directionality. However, none of these physical changes was altered by SOCS3 knockdown, and so pathways controlling initial contact with macrophages are not the main target but rather, events associated with speed and efficiency of uptake. This was highlighted by the observations that the uptake rates increased after engulfment of the first particle in SOCS3-silenced macrophages and that postengulfment processing and phagosome maturation were delayed. These enhanced kinetics could account for the greater number of beads and neutrophils engulfed overall in SOCS3-silenced cells.

Apoptotic cell uptake is controlled by a complex network of signaling pathways. PI3K activity is a critical for protrusion of the plasma membrane during phagocytic cup formation and for phagosomal closure [11]. The PI3K products, p-Akt and phosphatidylinositol 3,4,5-triphosphate, promote efficient uptake of apoptotic cells. Previous studies, including our own, have shown the ability of SOCS3 to inhibit PI3K-mediated signaling in other biologic contexts, including inflammatory responses [18, 35–37]. This also appears to be the case in bead-activated macrophages, where we found SOCS3 inhibition significantly enhanced PI3K activity, and inhibition of PI3K prevented the enhanced phagocytosis in SOCS3-silenced cells. A limitation of these studies, however, is that the PI3K inhibitor, LY294002, resulted in a marginal decrease in basal phagocytosis. Therefore, if the LY294002-induced dampening of phagocytosis is downstream of SOCS3 and at the level of p-AKT activity, then the significant inhibition of phagocytosis observed in SOCS3 knockdown macrophages with this drug may not be entirely related to SOCS3 silencing per se. PI3K-dependent activation of Rac1 is also indispensable for cytoskeletal rearrangements and inducing membrane ruffling and lamellipodial extensions [11]. All forms of apoptotic cell uptake tested to date have a strict requirement for Rac1 for engulfment, including apoptotic cell

clearance by bronchial epithelial cells and clearance of dying cells by *Caenorhabditis elegans* [43, 44]. The up-regulation of Rac1 activity with SOCS3 knockdown further emphasizes the importance of SOCS3 in controlling this arm of the signaling pathway in phagocytosis, and overall, we propose that SOCS3 modulation of PI3K, Rac1, and actin cytoskeletal arrangements is key to this process. However, it is also plausible that SOCS3 inhibits phagocytosis by synergizing with other mechanisms. FAK is a key tyrosine kinase linking integrins to downstream Rac-specific guanine nucleotide exchange factors, which in turn, regulate actin polymerization or turnover to induce particle engulfment [45]. SOCS3 was found to inhibit FAK-associated kinase activity and FAK tyrosine phosphorylation [46]. SOCS proteins also promoted polyubiquitination and degradation of FAK in a SOCS box-dependent manner and inhibited FAK-dependent signaling events, such as cell motility on fibronectin. This may provide an alternative mode of action for SOCS3 in controlling phagocytic uptake, although FAK activation is not a main pathway driving apoptotic cell uptake in resolution of inflammation. SOCS3 inhibits STAT3 activation, and deficiency in myeloid lineage cells has been shown to prolong activation of STAT3 [17–19]. Inhibition of STAT3 signaling also results in a decreased clearance of apoptotic cells [42, 47], thus SOCS3, by inhibiting STAT3, could potentially regulate cell uptake through this mechanism. However, SOCS3 specifically inhibits gp130-induced STAT3 activation, and whether this is operational during the uptake process requires further study.

Organized actin polymerization at the phagosome is pivotal for engulfment [6, 10, 11]. We evaluated the functional effect of SOCS3 knockdown on the distribution of F-actin using live-cell imaging. It is striking that SOCS3-silenced cells appeared to show a greater cell area and a more organized appearance of actin fibers. The greater membrane area and polarized actin distribution is conducive to the enhanced uptake of particles observed in our studies and would be downstream of effects on PI3K and Rac1 [48].

SOCS3 can selectively control multiple pathways to fine tune macrophage proinflammatory properties [17–20]. We also show here that in the absence of SOCS3, M1-activated human macrophages default to a less-proinflammatory phenotype, as determined by gene-expression analysis. This is in line with our previously published results showing changes in inflammatory mediators (TNF, IL-1β, IL-6, IL-12p70, IL-23, SOCS1, and HLA-DR) in IFN-γ/LPS-activated SOCS3 knockdown macrophages at the protein level [17, 18]. The exact mechanisms relating to this were not addressed in the present study, but we [17, 18] and others [19, 20] have previously shown that in SOCS3 knockout and knockdown rodent M1-activated macrophages, the decrease in inflammatory functions especially relates to changes in STAT3; PI3K (increased and anti-inflammatory); and NF-κB, MAPK, and Notch signaling (decreased and proinflammatory). Moreover, when Notch signaling was blocked, M1 stimuli induced a M2 response, and it was proposed that this was a result of the downstream effects on SOCS3 [20]. TNF expression was down-regulated with SOCS3 silencing, and this cytokine is known to block M2 polarization in a gene-specific way, providing an alternative mechanism by which SOCS3 controls activation [49]. The alteration in phenotypic markers in SOCS3 knockdown

human macrophages is in contrast to results in M1-activated macrophages obtained from myeloid-specific SOCS3-deficient mice [19], where SOCS3 deficiency enhanced expression of selected proinflammatory cytokine genes, in spite of enhanced STAT3 activation; the effect on M2 gene expression was not, however, determined. The reasons for the discrepancy in findings are unclear but could relate to differences in LPS concentration, timing of mRNA isolation after stimulation, and importantly, technologies and species used, for example, siRNA-mediated knockdown in rodent and human macrophages versus bone marrow cells from myeloid-specific SOCS3 knockout mice.

In summary, our results provide a novel mechanistic insight into the role of SOCS3 in primary human macrophages, suggesting that SOCS3 not only drives macrophage inflammatory responses but also controls pathways involved in actin remodeling to regulate the efficiency of phagocytic events. Thus, SOCS3 expression has dual effects relevant to the resolution of injury or infection. Therefore, strategies for SOCS3 modulation offer an opportunity for pharmacological targeting to both restrict inflammatory responses and additionally, to accelerate phagocytic clearance and resolution of inflammation in diseases, such as atherosclerotic plaques, where both inflammation and defective clearance of apoptotic cells play a significant part [9].

AUTHORSHIP

P.G., B.O., and J.I.H. were responsible for the study design and data acquisition, analysis, and interpretation. L.P.E. designed experiments and provided intellectual input. H.M.W. designed experiments, provided supervision, analyzed data, and wrote the manuscript. All authors were involved in drafting the article or revising it critically for important intellectual content, and all authors read and approved the final manuscript.

ACKNOWLEDGMENTS

DISCLOSURES

The authors declare no conflicts of interest.

REFERENCES

1. Murray, P. J., Wynn, T. A. (2011) Protective and pathogenic functions of macrophage subsets. *Nat. Rev. Immunol.* **11,** 723–737.
2. Martinez, F. O., Sica, A., Mantovani, A., Locati, M. (2008) Macrophage activation and polarization. *Front. Biosci.* **13,** 453–461.
3. Murray, P. J., Allen, J. E., Biswas, S. K., Fisher, E. A., Gilroy, D. W., Goerdt, S., Gordon, S., Hamilton, J. A., Ivashkiv, L. B., Lawrence, T., Locati, M., Mantovani, A., Martinez, F. O., Mege, J. L., Mosser, D. M., Natoli, G., Saeij, J. P., Schultze, J. L., Shirey, K. A., Sica, A., Suttles, J., Udalova, I., van Ginderachter, J. A., Vogel, S. N., Wynn, T. A. (2014) Macrophage activation and polarization: nomenclature and experimental guidelines. *Immunity* **41,** 14–20.

4. Poon, I. K., Lucas, C. D., Rossi, A. G., Ravichandran, K. S. (2014) Apoptotic cell clearance: basic biology and therapeutic potential. *Nat. Rev. Immunol.* **14,** 166–180.

5. Erwig, L. P., Henson, P. M. (2007) Immunological consequences of apoptotic cell phagocytosis. *Am. J. Pathol.* **171,** 2–8.

6. Erwig, L. P., Henson, P. M. (2008) Clearance of apoptotic cells by phagocytes. *Cell Death Differ.* **15,** 243–250.

7. Erwig, L. P., McPhilips, K. A., Wynes, M. W., Ivetic, A., Ridley, A. J., Henson, P. M. (2006) Differential regulation of phagosome maturation in macrophages and dendritic cells mediated by Rho GTPases and ezrin-radixin-moesin (ERM) proteins. *Proc. Natl. Acad. Sci. USA* **103,** 12825–12830.

8. Fadok, V. A., Bratton, D. L., Konowal, A., Freed, P. W., Westcott, J. Y., Henson, P. M. (1998) Macrophages that have ingested apoptotic cells in vitro inhibit proinflammatory cytokine production through autocrine/paracrine mechanisms involving TGF-beta, PGE2, and PAF. *J. Clin. Invest.* **101,** 890–898.

9. Thorp, E., Tabas, I. (2009) Mechanisms and consequences of efferocytosis in advanced atherosclerosis. *J. Leukoc. Biol.* **86,** 1089–1095.

10. Gumienny, T. L., Brugnera, E., Tosello-Trampont, A. C., Kinchen, J. M., Haney, L. B., Nishiwaki, K., Walk, S. F., Nemergut, M. E., Macara, I. G., Francis, R., Schedl, T., Qin, Y., Van Aelst, L., Hengartner, M. O., Ravichandran, K. S. (2001) CED-12/ELMO, a novel member of the CrkII/Dock180/Rac pathway, is required for phagocytosis and cell migration. *Cell* **107,** 27–41.

11. Leverrier, Y., Ridley, A. J. (2001) Requirement for Rho GTPases and PI 3-kinases during apoptotic cell phagocytosis by macrophages. *Curr. Biol.* **11,** 195–199.

12. Wilson, H. M. (2014) SOCS proteins in macrophage polarization and function. *Front. Immunol.* **5,** 357–361.

13. Strebovsky, J., Walker, P., Dalpke, A. H. (2012) Suppressor of cytokine signaling proteins as regulators of innate immune signaling. *Front. Biosci. (Landmark Ed.)* **17,** 1627–1639.

14. Dalpke, A., Heeg, K., Bartz, H., Baetz, A. (2008) Regulation of innate immunity by suppressor of cytokine signaling (SOCS) proteins. *Immunobiology* **213,** 225–235.

15. Chong, M. M., Metcalf, D., Jamieson, E., Alexander, W. S., Kay, T. W. (2005) Suppressor of cytokine signaling-1 in T cells and macrophages is critical for preventing lethal inflammation. *Blood* **106,** 1668–1675.

16. Whyte, C. S., Bishop, E. T., Rückerl, D., Gaspar-Pereira, S., Barker, R. N., Allen, J. E., Rees, A. J., Wilson, H. M. (2011) Suppressor of cytokine signaling (SOCS)1 is a key determinant of differential macrophage activation and function. *J. Leukoc. Biol.* **90,** 845–854.

17. Liu, Y., Stewart, K. N., Bishop, E., Marek, C. J., Kluth, D. C., Rees, A. J., Wilson, H. M. (2008) Unique expression of suppressor of cytokine signaling 3 is essential for classical macrophage activation in rodents in vitro and in vivo. *J. Immunol.* **180,** 6270–6278.

18. Arnold, C. E., Whyte, C. S., Gordon, P., Barker, R. N., Rees, A. J., Wilson, H. M. (2014) A critical role for suppressor of cytokine signalling 3 in promoting M1 macrophage activation and function in vitro and in vivo. *Immunology* **141,** 96–110.

19. Qin, H., Holdbrooks, A. T., Liu, Y., Reynolds, S. L., Yanagisawa, L. L., Benveniste, E. N. (2012) SOCS3 deficiency promotes M1 macrophage polarization and inflammation. *J. Immunol.* **189,** 3439–3448.

20. Wang, Y. C., He, F., Feng, F., Liu, X. W., Dong, G. Y., Qin, H. Y., Hu, X. B., Zheng, M. H., Liang, L., Feng, L., Liang, Y. M., Han, H. (2010) Notch signaling determines the M1 versus M2 polarization of macrophages in antitumor immune responses. *Cancer Res.* **70,** 4840–4849.

21. Labuzek, K., Suchy, D., Gabryel, B., Pierzchała, O., Okopień, B. (2012) Role of the SOCS in monocytes/macrophages-related pathologies. Are we getting closer to a new pharmacological target? *Pharmacol. Rep.* **64,** 1038–1054.

22. Marine, J. C., Topham, D. J., McKay, C., Wang, D., Parganas, E., Stravopodis, D., Yoshimura, A., Ihle, J. N. (1999) SOCS1 deficiency causes a lymphocyte-dependent perinatal lethality. *Cell* **98,** 609–616.

23. Starr, R., Metcalf, D., Elefanty, A. G., Brysha, M., Willson, T. A., Nicola, N. A., Hilton, D. J., Alexander, W. S. (1998) Liver degeneration and lymphoid deficiencies in mice lacking suppressor of cytokine signaling-1. *Proc. Natl. Acad. Sci. USA* **95,** 14395–14399.

24. Brysha, M., Zhang, J.-G., Bertolino, P., Corbin, J. E., Alexander, W. S., Nicola, N. A., Hilton, D. J., Starr, R. (2001) Suppressor of cytokine signaling-1 attenuates the duration of interferon γ signal transduction in vitro and in vivo. *J. Biol. Chem.* **276,** 22086–22089.

25. Lang, R., Pauleau, A. L., Parganas, E., Takahashi, Y., Mages, J., Ihle, J. N., Rutschman, R., Murray, P. J. (2003) SOCS3 regulates the plasticity of gp130 signaling. *Nat. Immunol.* **4,** 546–550.

26. Croker, B. A., Krebs, D. L., Zhang, J. G., Wormald, S., Willson, T. A., Stanley, E. G., Robb, L., Greenhalgh, C. J., Förster, I., Clausen, B. E., Nicola, N. A., Metcalf, D., Hilton, D. J., Roberts, A. W., Alexander, W. S. (2003) SOCS3 negatively regulates IL-6 signaling in vivo. *Nat. Immunol.* **4,** 540–545.

27. Yasukawa, H., Ohishi, M., Mori, H., Murakami, M., Chinen, T., Aki, D., Hanada, T., Takeda, K., Akira, S., Hoshijima, M., Hirano, T., Chien, K. R., Yoshimura, A. (2003) IL-6 induces an anti-inflammatory response in the absence of SOCS3 in macrophages. *Nat. Immunol.* **4,** 551–556.

28. Dimitriou, I. D., Clemenza, L., Scotter, A. J., Chen, G., Guerra, F. M., Rottapel, R. (2008) Putting out the fire: coordinated suppression of the innate and adaptive immune systems by SOCS1 and SOCS3 proteins. *Immunol. Rev.* **224,** 265–283.

29. White, G. E., Cotterill, A., Addley, M. R., Soilleux, E. J., Greaves, D. R. (2011) Suppressor of cytokine signalling protein SOCS3 expression is increased at sites of acute and chronic inflammation. *J. Mol. Histol.* **42,** 137–151.

30. Okai, B., Lyall, N., Gow, N. A., Bain, J. M., Erwig, L. P. (2015) Rab14 regulates maturation of macrophage phagosomes containing the fungal pathogen *Candida albicans* and outcome of the host-pathogen interaction. *Infect. Immun.* **83,** 1523–1535.

31. Lukinavičius, G., Reymond, L., D'Este, E., Masharina, A., Göttfert, F., Ta, H., Güther, A., Fournier, M., Rizzo, S., Waldmann, H., Blaukopf, C., Sommer, C., Gerlich, D. W., Arndt, H.-D., Hell, S. W., Johnsson, K. (2014) Fluorogenic probes for live-cell imaging of the cytoskeleton. *Nat. Methods* **11,** 731–733.

32. Korns, D., Frasch, S. C., Fernandez-Boyanapalli, R., Henson, P. M., Bratton, D. L. (2011) Modulation of macrophage efferocytosis in inflammation. *Front. Immunol.* **2,** 57.

33. Underhill, D. M., Goodridge, H. S. (2012) Information processing during phagocytosis. *Nat. Rev. Immunol.* **12,** 492–502.

34. Canton, J. (2014) Phagosome maturation in polarized macrophages. *J. Leukoc. Biol.* **96,** 729–738.

35. O'Connor, J. C., Sherry, C. L., Guest, C. B., Freund, G. G. (2007) Type 2 diabetes impairs insulin receptor substrate-2-mediated phosphatidylinositol 3-kinase activity in primary macrophages to induce a state of cytokine resistance to IL-4 in association with overexpression of suppressor of cytokine signaling-3. *J. Immunol.* **178,** 6886–6893.

36. Metlakunta, A. S., Sahu, M., Yasukawa, H., Dhillon, S. S., Belsham, D. D., Yoshimura, A., Sahu, A. (2011) Neuronal suppressor of cytokine signaling-3 deficiency enhances hypothalamic leptin-dependent phosphatidylinositol 3-kinase signaling. *Am. J. Physiol. Regul. Integr. Comp. Physiol.* **300,** R1185–R1193.

37. Ueki, K., Kondo, T., Kahn, C. R. (2004) Suppressor of cytokine signaling 1 (SOCS-1) and SOCS-3 cause insulin resistance through inhibition of tyrosine phosphorylation of insulin receptor substrate proteins by discrete mechanisms. *Mol. Cell. Biol.* **12,** 5434–5446.

38. Castellano, F., Montcourrier, P., Chavrier, P. (2000) Membrane recruitment of Rac1 triggers phagocytosis. *J. Cell Sci.* **113,** 2955–2961.

39. Frasch, S. C., Fernandez-Boyanapalli, R. F., Berry, K. Z., Leslie, C. C., Bonventre, J. V., Murphy, R. C., Henson, P. M., Bratton, D. L. (2011) Signaling via macrophage G2A enhances efferocytosis of dying neutrophils by augmentation of Rac activity. *J. Biol. Chem.* **286,** 12108–12122.

40. Savill, J., Dransfield, I., Gregory, C., Haslett, C. (2002) A blast from the past: clearance of apoptotic cells regulates immune responses. *Nat. Rev. Immunol.* **2,** 965–975.

41. McPhillips, K., Janssen, W. J., Ghosh, M., Byrne, A., Gardai, S., Remigio, L., Bratton, D. L., Kang, J. L., Henson, P. (2007) TNF-alpha inhibits macrophage clearance of apoptotic cells via cytosolic phospholipase A2 and oxidant-dependent mechanisms. *J. Immunol.* **178,** 8117–8126.

42. Soki, F. N., Koh, A. J., Jones, J. D., Kim, Y. W., Dai, J., Keller, E. T., Pienta, K. J., Atabai, K., Roca, H., McCauley, L. K. (2014) Polarization of prostate cancer-associated macrophages is induced by milk fat globule-EGF factor 8 (MFG-E8)-mediated efferocytosis. *J. Biol. Chem.* **289,** 24560–24572.

43. Juncadella, I. J., Kadl, A., Sharma, A. K., Shim, Y. M., Hochreiter-Hufford, A., Borish, L., Ravichandran, K. S. (2013) Apoptotic cell clearance by bronchial epithelial cells critically influences airway inflammation. *Nature* **493,** 547–551.

44. Neukomm, L. J., Frei, A. P., Cabello, J., Kinchen, J. M., Zaidel-Bar, R., Ma, Z., Haney, L. B., Hardin, J., Ravichandran, K. S., Moreno, S., Hengartner, M. O. (2011) Loss of the RhoGAP SRGP-1 promotes the clearance of dead and injured cells in *Caenorhabditis elegans*. *Nat. Cell Biol.* **13,** 79–86.

45. Finnemann, S. C. (2003) Focal adhesion kinase signaling promotes phagocytosis of integrin-bound photoreceptors. *EMBO J.* **22,** 4143–4154.

46. Liu, E., Côté, J. F., Vuori, K. (2003) Negative regulation of FAK signaling by SOCS proteins. *EMBO J.* **22,** 5036–5046.

47. Aziz, M., Jacob, A., Matsuda, A., Wu, R., Zhou, M., Dong, W., Yang, W. L., Wang, P. (2011) Pre-treatment of recombinant mouse MFG-E8 downregulates LPS-induced TNF-α production in macrophages via STAT3-mediated SOCS3 activation. *PLoS One* **6,** e27685.

48. Bain, J. M., Louw, J., Lewis, L. E., Okai, B., Walls, C. A., Ballou, E. R., Walker, L. A., Reid, D., Munro, C. A., Brown, A. J., Brown, G. D., Gow, N. A., Erwig, L. P. (2014) *Candida albicans* hypha formation and mannan masking of β-glucan inhibit macrophage phagosome maturation. *MBio* **5,** e01874.

49. Kratochvill, F., Neale, G., Haverkamp, J. M., Van de Velde, L. A., Smith, A. M., Kawauchi, D., McEvoy, J., Roussel, M. F., Dyer, M. A., Qualls, J. E., Murray, P. J. (2015) TNF counterbalances the emergence of M2 tumor macrophages. *Cell Reports* **12,** 1902–1914.

Supplemental Material	http://www.jleukbio.org/content/suppl/2016/04/20/jlb.3A1215-554RR.DC1.html
References	This article cites 49 articles, 19 of which can be accessed free at: http://www.jleukbio.org/content/100/4/771.full.html#ref-list-1
Subscriptions	Information about subscribing to *Journal of Leukocyte Biology* is online at http://www.jleukbio.org/site/misc/Librarians_Resource.xhtml
Permissions	Submit copyright permission requests at: http://www.jleukbio.org/site/misc/Librarians_Resource.xhtml
Email Alerts	Receive free email alerts when new an article cites this article - sign up at http://www.jleukbio.org/cgi/alerts